Relationship Between Contact Inhibition and Intranuclear S100C of Normal Human Fibroblasts

Masakiyo Sakaguchi,* Masahiro Miyazaki,* Yusuke Inoue,* Toshiya Tsuji,* Hirosuke Kouchi,* Toshio Tanaka,‡ Hidenori Yamada,§ and Masayoshi Namba*

*Department of Cell Biology, Institute of Molecular and Cellular Biology, Okayama University Medical School, Okayama 700-8558, Japan; ‡Department of Molecular and Cellular Pharmacology, Mie University, Mie 514-8507, Japan; and §Department of Bioscience and Biotechnology, Faculty of Engineering, Okayama University, Okayama 700-8530, Japan

Abstract. Many lines of evidence indicate that neoplastic transformation of cells occurs by a multistep process. For neoplastic transformation of normal human cells, they must be first immortalized and then be converted into neoplastic cells. It is well known that the immortalization is a critical step for the neoplastic transformation of cells and that the immortal phenotype is recessive. Thus, we investigated proteins downregulated in immortalized cells by two-dimensional gel electrophoresis. As a result, S100C, a Ca^{2+}-binding protein, was dramatically downregulated in immortalized human fibroblasts compared with their normal counterparts. When the cells reached confluence, S100C was phosphorylated on threonine 10. Then the phosphorylated S100C moved to and accumulated in the nuclei of normal cells, whereas in immortalized cells it was not phosphorylated and remained in the cytoplasm. Microinjection of the anti-S100C antibody into normal confluent quiescent cells induced DNA synthesis. Furthermore, when exogenous S100C was compelled to localize in the nuclei of HeLa cells, their DNA synthesis was remarkably inhibited with increase in cyclin-dependent kinase inhibitors such as $p16^{Ink4a}$ and $p21^{Waf1}$. These data indicate the possible involvement of nuclear S100C in the contact inhibition of cell growth.

Key words: immortalization of human cells • S100C protein • actin filaments • nuclear import • cell density–dependent growth arrest

Introduction

Many lines of evidence indicate that neoplastic transformation of cells occurs by a multistep process, which is clearly determined by the successive stages of aging, immortalization, and neoplastic transformation (Namba et al., 1996; Hayflick, 1997). It is well known that normal human diploid cells are extremely refractory to in vitro neoplastic transformation, because they cannot be easily immortalized. Once they are immortalized, they can easily undergo neoplastic transformation by treatment with carcinogenic agents, including chemicals, radiation, and oncogenes (Rhim et al., 1990; Namba et al., 1996). These facts indicate that cellular immortalization is an important early step of human carcinogenesis. However, the molecular mechanism responsible for cellular immortalization is still poorly understood.

Two-dimensional (2-D)[1] PAGE is one of the powerful techniques for analyzing protein dynamics under various physiological conditions of cells. In this study, we used the 2-D PAGE technique to investigate the protein dynamics in normal and immortalized human fibroblasts in order to understand the mechanisms of cellular immortalization. We found that S100C (S100A11, calgizzarin: pI 6.2, molecular mass 11 kD) was dramatically downregulated in immortalized human fibroblasts as compared with their normal counterparts.

S100C is a member of EF-hand type Ca^{2+}-binding protein of the S100 family and was first identified in chicken gizzard smooth muscle and has also been detected in several mammalian species and tissues (Watanabe et al., 1991; Tanaka et al., 1995; Schnekess and Walsh, 1997). It has

Address correspondence to Masayoshi Namba, Department of Cell Biology, Institute of Molecular and Cellular Biology, Okayama University Medical School, 2-5-1 Shikata, Okayama 700-8558, Japan. Tel.: 81-86-235-7393. Fax: 81-86-235-7400. E-mail: mnamba@med.okayama-u.ac.jp

[1]*Abbreviations used in this paper:* 2-D, two-dimensional; BrdU, bromodeoxyuridine; CBB, Coomassie brilliant blue; GST, glutathione *S*-transferase; NLS, nuclear localization signal; PVDF, polyvinylidene difluoride filter.

been suggested that the S100 family, including S100C, plays important roles in cell cycle regulation, differentiation, growth, and metabolic control (Allen et al., 1996; Marti et al., 1996; Scotto et al., 1998). Many studies have been carried out to determine the functions of S100C in vivo and in vitro; however, little is known about its precise intracellular functions. The purpose of this study was to investigate the biological functions of S100C in normal human fibroblasts and their immortalized cells.

Materials and Methods

Cell Culture, ^{32}P Labeling, Bromodeoxyuridine (BrdU) Labeling, and [^3H]Thymidine Incorporation

Normal human fibroblast strains (KMS-6, OUMS-36, and OUMS-24) and their immortalized cell lines (KMST-6, SUSM-1, and OUMS-24F) were cultured in a 5% CO_2 incubator at 37°C. MEM (Nissui) supplemented with 10% FBS (Intergen Co.) was used. Characteristics of these cell lines have been described elsewhere (Namba et al., 1985, 1988; Bai et al., 1993). ^{32}P labeling of cells was performed as described previously (Kondo et al., 1995). In brief, cells were incubated in a phosphate-free medium for 2 h and then labeled with [^{32}P]orthophosphate at a dose of 100 mCi/ml (ICN) at 37°C for 6 h. For phosphorylation of recombinant S100C in a cell-free system, confluent normal KMS-6 cell pellets were lysed in 500 μl of detergent disruption buffer (0.5% NP-40, 2.5 mM DTT, 15% glycerol, 1 mM NaF, 0.1 mM Na_3VO_4, 135 mM KCl, 100 μM $CaCl_2$, 1 μg/ml leupeptin, 1 μg/ml aprotinin, 50 mM Tris-HCl, pH 7.4). Supernatants were separated by a 20-min centrifugation at 15,000 rpm, and protein contents were adjusted to 1 mg/ml. Purified recombinant glutathione *S*-transferase (GST)-S100C (1 μg) and [γ-^{32}P]ATP (1 μCi) were added to the supernatants and incubated for 25 min at 25°C. ^{32}P-labeled GST-S100C in cell lysates was obtained by glutathione-agarose affinity chromatography. ^{32}P-labeled S100C was cut off by treatment of the ^{32}P-labeled GST-S100C with bovine thrombin and then subjected to the SDS-PAGE. DNA synthesis was assessed by BrdU (Sigma) (Dover and Patel, 1994) or [^3H]thymidine uptake. Detection of the BrdU was carried out using mouse anti-BrdU antibody (Neomarkers) as the primary antibody and FITC-conjugated goat anti–mouse IgG antibody (Sigma) as the secondary antibody. To assay [^3H]thymidine incorporation, trypsinized cells were plated in 24-well plates at a density of 5×10^4 cells/ml and cultured overnight at 37°C in MEM supplemented with 10% tetracycline system-approved FBS (CLONTECH Laboratories, Inc.) and doxycycline (1 μg/ml). Then, the medium was replaced with the fresh medium containing no doxycycline, and the cells were further incubated for 3–12 h. Tritiated thymidine (1 μCi/ml; ART) was added to the cultures 3 h before cell harvest.

Expression Vectors

The procaryote expression plasmid pGEX-2T-S100C was constructed to express a GST-S100C fusion protein by inserting the cDNA of human S100C into the pGEX-2T vector (Naka et al., 1994). To delete the phosphorylation site of S100C protein, three mutant expression plasmids (pGEX-2T 8-10 A/T S100C, 8 A/T S100C, and 10 A/T S100C) were constructed to express various S100C protein homologues (8-10 A/T, 8 A/T, and 10 A/T). A total of 10 primers (CCAGCCCTGCAGAGGCTGAGCGGTGC; T8-10-A F, CTCCAGCCCTGCAGAGACTG; T8-A F, CCAGCCCTACAGAGGCTGAGCGGTGC; T10-A F, TATAGCATGGCCTTTGCAGGG; GST F as 5′-primers; and GCACCGCTCAGCCTCTGCAGGGCTGG; T8-10-A R, CAGTCTCTGCAGGGCTGGAG; T8-A R, GCACCGCTCAGCCTCTGTAGGGCTGG; T10-A R, ATTCATGAAGCTTAGGAACTC; HindR as 3′-downstream primers) were used. Three sets of PCR products (T8-10-A F/HindR and T8-10-A R/GST F; T8-A F/HindR and T8-A R/GST F; T10-A F/HindR and T10-A R/GST F) were synthesized on a pGEX-2T-S100C template by first PCR, and they were then religated by second PCR using the 5′-primer GST F and the 3′-downstream primer HindR. These fragments were inserted into the BamH1/HindIII site of pGEX-2T-S100C plasmid. Nucleotide sequences of these mutant S100C expression vectors were confirmed by direct sequencing. The human S100C expression plasmid pTracer-EF-A-S100C was constructed to overexpress S100C in cells. A 306-bp NotI-NotI fragment was obtained by PCR of pGEX-2T-S100C vector using a 5′-primer (GCGGCCGCATGGCAAAAATCTCCAGC) and a 3′-downstream primer (GCGGCCGCTCAGGTCCGCTTCTGGGA). The fragment containing the open reading frame of the human *S100C* gene was ligated to the NotI site of the eukaryote expression vector pTracer-EF-A (Invitrogen). The pTRE S100C–nuclear localization signal (NLS) vector was constructed to specifically localize S100C-NLS fusion protein in the nucleus. Human S100C cDNA linked to simian virus 40 large T antigen NLS (PKKKRKV) cDNA was obtained by PCR of pGEX-2T-S100C vector using a 5′-primer (CTCAGCTCCAACATGGCAAA) and a 3′-downstream primer (TTATACCTTTCTCTTCTTTTTTGGGGTCCGCTTCTGGGAAGGGA). S100C-NLS cDNA was subcloned into the pGEM-T easy cloning vector (Promega) and restricted by EcoRI. The fragment was ligated to EcoRI site of the pTRE cloning vector. The pTRE S100C vector was also constructed. The EcoRI restricted fragments of the pGEM-T vector containing S100C cDNA was ligated to a pTRE cloning vector. Nucleotide sequences of these S100C expression vectors were confirmed by DNA sequencing.

Transfection

Tet-off HeLa cell line (Clontech) was doubly transfected with pTRE S100C or pTRE S100C-NLS and pSV2-Hyg selection vector carrying hygromycin B resistance gene (ratio, 10:1) by lipofection using Lipofectamine (GIBCO BRL) according to the manufacturer's instructions. After 48 h, stably transfected clones were selected by hygromycin B (200 μg/ml) in MEM supplemented with 10% Tet system approved FBS (Clontech) and doxycycline (1 μg/ml).

2-D Gel Electrophoresis

Protein sampling and isoelectric focusing separation with immobilized pH gradient (pH, 4.0–7.0) gels (IPG; Amersham Pharmacia Biotech) were performed as described previously (Kondo et al., 1998a). After equilibration with SDS, the IPG gels were placed directly onto 15% tricine SDS-polyacrylamide slab gels and run with a vertical electrophoresis system (Nihon Eido). Owing to the nature of this system, we used two types of running buffer for electrophoresis, i.e., a top running buffer (0.1 M tricine, 0.1% SDS, 0.1 M Tris, pH 8.2) as a cathode and a bottom running buffer (0.2 M Tris, pH 8.9) as an anode.

Protein Sequencing

Coomassie brilliant blue (CBB)-stained protein on a polyvinylidene difluoride filter (PVDF) membrane was digested with 1 pmol of lysyl endopeptidase (*Achromobacter protease* I; WAKO). Some peptide fragments eluted from the PVDF membrane were separated on a C18 column (YMC-pack ODS-A, 150 mm × 6.0 mm ID; Amersham Pharmacia Biotech) by HPLC, with monitoring of their absorbance at 210 nm. The separated peptides were subjected to NH_2-terminal sequencing on a Model 491 peptide sequencer (Applied Biosystems). For NH_2-terminal sequencing of phosphopeptide, the spot of phosphopeptide on a TLC plate was scraped off and extracted with electrophoresis buffer (formic acid/acetic acid/double-distilled water (DDW), 1:3:16). After drying the extract, the dried sample was moistened by SDS sample buffer, subjected to tricine SDS-PAGE, and blotted onto a PVDF membrane. The peptide band was cut off from the CBB-stained PVDF membrane, and the peptide sequence was analyzed by the peptide sequencer.

Antibody to Recombinant Human S100C Protein

Escherichia coli (*E. coli* NM 522) cells were transformed by the procaryote expression vector pGEX-2T-S100C. Purification of the GST-S100C fusion protein in transformed cell extracts was performed by glutathione-agarose affinity chromatography using a Sephadex 4B column (Amersham Pharmacia Biotech). After dialysis of the GST-S100C fraction with a dialysis buffer (150 mM NaCl, 1.5 mM KCl, 20 mM Tris, pH 7.4), bovine thrombin was added to the GST-S100C solution at a concentration of 1:200 (wt/wt). The mixture was incubated at 37°C for 60 min to complete the proteolysis reaction, and then S100C protein was isolated from the protein mixture by chromatography with a Sephadex 4B column. For preparation of anti–human S100C antibody, rabbits were immunized three times for 2 mo with the human recombinant S100C (each at 1 mg per animal). Immune serum was collected from each rabbit and the IgG fraction was isolated by salting-out. We confirmed that anti-S100C antibody reacted specifically with human S100C (11 kD) on Western blot.

Immunocytochemistry

To visualize S100C and actin filaments simultaneously, cells were treated with rabbit anti-S100C antibody at 37°C for 1 h and treated with BODIPY 558/568–conjugated phalloidin (a specific probe for actin filaments; Molecular Probes, Inc.) under the same conditions reported previously (Sakaguchi et al., 1998, 1999; Kondo et al., 1998b). Then, cells were treated at 37°C for 1 h with a secondary antibody and FITC-conjugated goat anti-rabbit IgG antibody (Sigma).

Immunostaining of Exogenously Added S100C

Total cell extracts were prepared by homogenizing normal and immortalized cells at various stages in a homogenizing buffer (10 mM KCl, 3 mM ATP, 5 mM $MgCl_2$, 10 μg/ml leupeptin, 10 μg/ml aprotinin, and 200 μg/ml phenylmethanesulfonyl fluoride, 10 mM Hepes, pH 7.0). Confluent normal and immortalized cells on coverslips were permeabilized with digitonin (Mishra and Parnaik, 1995; Yokoya et al., 1999) and then incubated with normal or immortalized cell extracts that were treated with or not treated with alkaline phosphatase from *Escherichia coli* (WAKO) at 37°C for 15 min. Thereafter, the cells were immunostained for S100C as described above.

Immunoprecipitation and Immunoblotting

Total cell lysates were prepared from normal and immortalized cells at various stages with a cell lysis buffer (300 mM NaCl, 1% Triton X-100, 1 mM $CaCl_2$, 10 μg/ml leupeptin, 10 μg/ml aprotinin, and 200 μg/ml phenylmethanesulfonyl fluoride, 10 mM Tris, pH 7.3). Subfractionation of the total cell lysates was carried out basically as described previously (Lindeman et al., 1997). In brief, the total cell lysates, soluble, and nuclear fractions were cleared by treatment with excess of protein A–Sepharose (Sigma). Cleared cell samples were incubated with rabbit anti-S100C antibody at 4°C for 60 min followed by protein A, and the immunoprecipitates were resolved on tricine SDS-PAGE and transferred onto nitrocellulose membranes (Amersham Pharmacia Biotech). Immunoblotting of the membranes was performed as reported previously (Sakaguchi et al., 1999) using rabbit anti-S100C antibody or rabbit anti-actin antibody followed by HRP-conjugated goat anti–rabbit IgG antibody (MBL). Then, S100C and actin were detected by the enhanced chemiluminescence system (Amersham Pharmacia Biotech). Native polyacrylamide gel electrophoretic analysis was performed as reported previously (Tom et al., 1996). In brief, the total cell lysates were resolved in 4% native polyacrylamide gels at 4°C and then immunoblotted with rabbit anti-S100C antibody as described above.

Cosedimentation Assay

To examine binding of S100C to purified actin filaments, a simple high-speed cosedimentation assay was performed as described previously (González et al., 1998). Purified monomeric actin (G-actin, 10 μM; Sigma) was incubated with recombinant GST-S100C (10 μM) or GST (10 μM) in an actin polymerization buffer (2 mM $MgCl_2$, 100 mM KCl, 0.1 mM ATP, 10 mM Hepes, pH 7.3) containing various concentrations of Ca^{2+} at room temperature for 60 min to complete actin polymerization. Association of recombinant S100C with polymerized actin filaments was determined by a sedimentation assay with ultracentrifugation at 126,000 *g* for 20 min in a Beckman Airfuge. Equal volumes of the pellet and supernatant from each reaction mixture were subjected to SDS-PAGE. The amounts of GST-S100C and actin were then quantified by densitometry of the stained gels.

DNase I Affinity Chromatography

Affi-Gel 10 (Bio-Rad) coupled with DNase I, which specifically binds to G-actin, was used to examine the interaction of G-actin with GST-S100C. G-Actin (10 μM)-bound DNase I affinity beads and various concentrations of GST-S100C (1–100 μM) in a hypoionic strength buffer (0.1 mM ATP, 10 mM Hepes, pH 7.3) were incubated for 2 h at room temperature in the presence of 1 mM Ca^{2+}. After the incubation, the beads were washed three times with the same buffer, resuspended in the electrophoresis sample buffer, and analyzed by SDS-PAGE.

2-D Separation of S100C Phosphopeptides

^{32}P-labeled phosphopeptide mapping was performed essentially as described previously, with a minor modification (Fackler et al., 1990). In brief, bands containing ^{32}P-labeled cellular S100C or recombinant S100C were excised from the dried SDS-polyacrylamide gel, rehydrated, and digested in 50 mM NH_4HCO_3 buffer, pH 8.3, containing lysyl endopeptidase for 16 h at 37°C. The ratio (mol/mol) of lysyl endopeptidase and S100C was 1:100. After centrifugation of the excised gel suspension, the supernatant was collected and lyophilized. The lyophilized sample was dissolved in 1 ml DDW and relyophilized. This process was repeated five times to completely remove NH_4HCO_3. The finally lyophilized samples were dissolved in 5 μl of electrophoresis buffer (formic acid/acetic acid/DDW, 1:3:16) and applied to thin layer plates (Amersham Pharmacia Biotech). Electrophoresis was carried out in the first dimension at 1,000 V for 30 min with cooling at 4°C. After drying, the plate was chromatographed for 3–4 h in the second dimension in n-butanol/pyridine/acetic acid/DDW (6.5:5:1:4) until the leading edge of the solvent had reached 1–2 cm from the top.

Phosphoamino Acid Analysis

Lysyl endopeptidase digests of ^{32}P-labeled intracellular S100C and recombinant S100C were incubated in 100 μl of 6 N HCl at 105°C for 60 min as described previously (Fackler et al., 1990). The samples were concentrated by a Speed Vac concentrator and dissolved in 5 μl of DDW containing standards (each 1 mg/ml of cold phosphoserine, phosphothreonine, and phosphotyrosine). Electrophoresis was carried out at 1,000 V for 50 min with cooling at 4°C using a pyridine/acetic acid/DDW (1:10:189) electrophoresis buffer. After drying the plates, the standards were identified with ninhydrin spray (Sigma). Then, ^{32}P-labeled phosphoamino acids were visualized by autoradiography.

Microinjection of S100C Expression Vector or Rabbit Anti–human S100C Antibody

The plasmid pTracer-EF-A-S100C was microinjected at a dose of 500 copies per nucleus into immortalized cells grown on coverslips. After 24 h, cells were fixed and observed under a fluorescence microscope. NBD fluoride (Molecular Probe), an amine reactive fluorescent probe, was conjugated with purified recombinant S100C according to the manufacturer's recommended protocol. The S100C-NBD fluoride (5 mg/ml) was microinjected into the cytoplasm of normal semiconfluent fibroblasts at a dose of 50 fl per cell, and the injected cells were incubated at 37°C for 2 h and then observed under a fluorescent microscope. For microinjection of rabbit anti-S100C antibody, normal cells were plated on coverslips. After reaching confluence, the cells were further maintained for 2 wk with three changes of the medium. After confirmation that the cells did not incorporate any BrdU, rabbit anti-S100C antibody (5 mg/ml) was microinjected into the cytoplasm at a dose of 50 fl per cell, and the injected cells were incubated at 37°C for 24 h. Localization of rabbit anti-S100C antibody in the injected cells was detected with TRITC-conjugated goat anti–rabbit IgG antibody (Sigma). Then, DNA synthesis in the injected cells was assessed by BrdU staining.

Results

S100C in Human Fibroblasts

In analysis using semiconfluent cells by 2-D gel electrophoresis, several hundred proteins were detected per silver-stained gel, and numerous differences in the protein expression levels were observed between normal and immortalized cells (Fig. 1 a). We noticed a spot of low–molecular weight protein that was downregulated in immortalized KMST-6 cells as compared with their normal counterparts (Fig. 1 a, arrows). The isoelectric point and molecular mass of the protein were 6.2 and 11 kD, respectively. The amino acid sequence of the protein was then determined. Nine peaks were obtained by HPLC separation of the lysyl endopeptidase digests, and four (Nos. 2, 3, 8, and 9) of them were sequenced (Fig. 1 b). At the top of Fig. 1 c, the sequences of the four peptides (Nos. 2, 3, 8, and 9) are shown. These sequences completely correspond to the underlined sequences of the full-length human

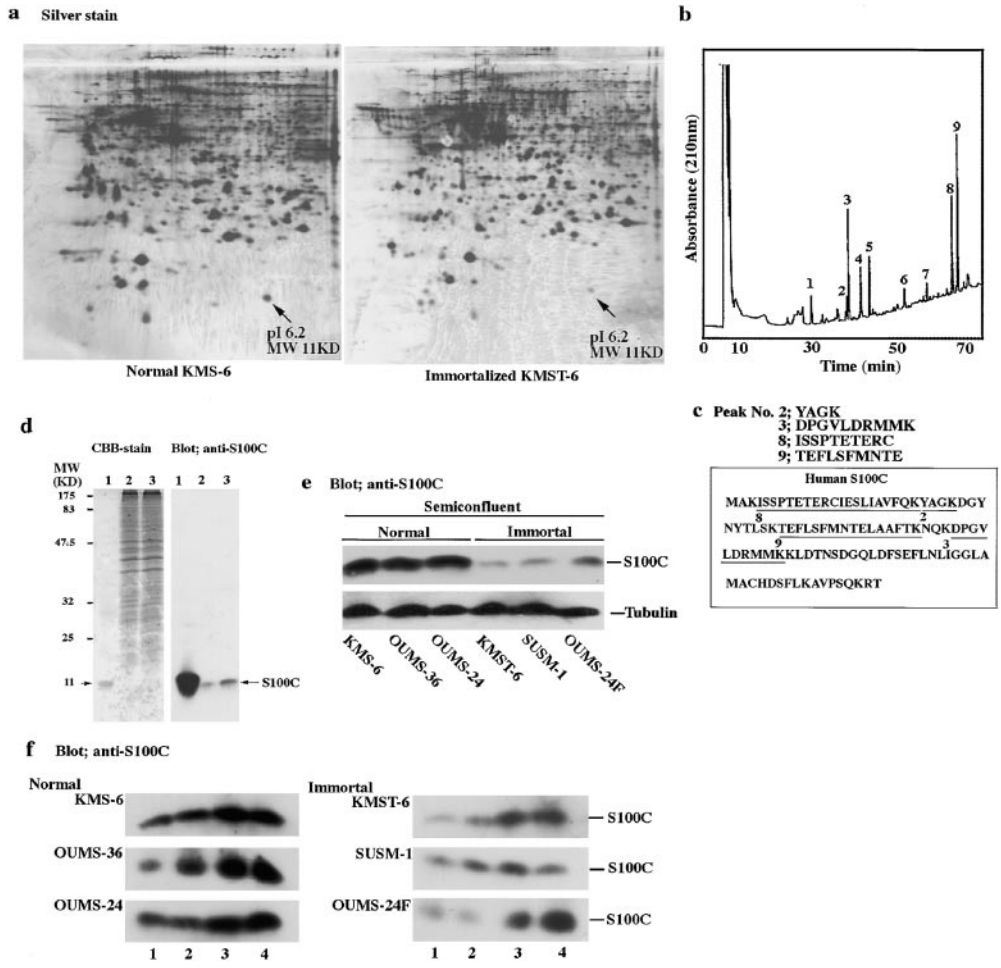

Figure 1. Identification of S100C in human fibroblasts. (a) 2-D gels of silver-stained proteins from normal human fibroblasts (KMS-6, left panel) and their immortalized counterparts (KMST-6, right panel). Arrows show a protein with a molecular mass of 11 kD and isoelectric point of 6.2. (b) Peptide mapping of this protein was performed by lysyl endopeptidase digestion and separation of cleavage products on reverse-phase HPLC using a C18 column. Nine major peptides were separated. (c) Amino acid sequences of four (Nos. 2, 3, 8, and 9) out of the nine peptides were determined. Underlined parts of full amino acid sequence of human S100C show consensus sequences of the four peptides. (d) Monospecificity of rabbit anti–human S100C antibody built up in this study was confirmed by Western blot analysis. (Left lanes) CBB staining. (Right lanes) Western blot of S100C: lane 1, 1 μg of recombinant human S100C; lanes 2 and 3, 30 and 60 μg of proteins from normal cells. (e) Comparison of S100C (upper) or tubulin (control, lower) expression levels in three normal (KMS-6, OUMS-36, OUMS-24) and three immortalized (KMST-6, SUSM-1, OUMS-24F) cells at low cell density by Western blot analysis using rabbit anti-S100C or anti-tubulin antibody. (f) After cells reached confluence, changes in amounts of S100C were assessed by Western blotting. (Left panel) Three normal cell strains (KMS-6, OUMS-36, OUMS-24). (Right panel) Three immortalized cell lines (KMST-6, SUSM-1, OUMS-24F): lane 1, semiconfluent stage; lanes 2–4, 24, 48, and 72 h after reaching confluence, respectively.

S100C (bottom of Fig. 1 c). As a result, the amino acid sequences of the four peptides were completely coincident with the partial sequence of human S100C protein (Fig. 1 c). Thus, we concluded that this protein was the human S100C protein.

To determine the biological functions of S100C, we built up a monospecific polyclonal antibody to human S100C (Fig. 1 d). Western blot analysis with the antibody showed that expression of the S100C protein was lower in immortalized fibroblast cell lines (KMST-6, SUSM-1, OUMS-24F) than in normal human fibroblast strains (KMS-6, OUMS-36, OUMS-24) at semiconfluence (Fig. 1 e). In addition, we found that the expression of the protein increased in parallel to cell density in both normal and immortalized cells (Fig. 1 f).

Localization of S100C in Cells

We next examined the subcellular distribution of S100C in normal and immortalized cells at low and high cell densities using the rabbit anti-S100C antibody. Immunoblot analyses showed that S100C was predominantly present in the soluble fractions from normal and immortalized cells at semiconfluence (Fig. 2 a). Interestingly, S100C accumulated in the nuclei of normal cells when they reached confluence, whereas it remained in the cytoplasm of immortalized cells even after confluence (Fig. 2 a). No difference in the cDNA sequence of S100C was observed between normal KMS-6 and immortalized KMST-6 cells (data not shown), indicating that different localization of S100C in normal and immortalized cells at confluence was not due to the *S100C* gene mutation.

Although it has been proposed that S100C can associate with actin cytoskeletal protein in vitro (Naka et al., 1994), it is still unclear whether the association actually occurred in human fibroblasts. For this point, the interaction between S100C and actin filaments in cells was further evaluated by GST fusion protein binding and immunoprecipitation assays. By loading extracts of normal and immortalized cells onto a column filled with glutathione beads coupled with GST-S100C fusion protein (Fig. 2 b, top right) or GST alone (Fig. 2 b, top left), we detected a protein with a mo-

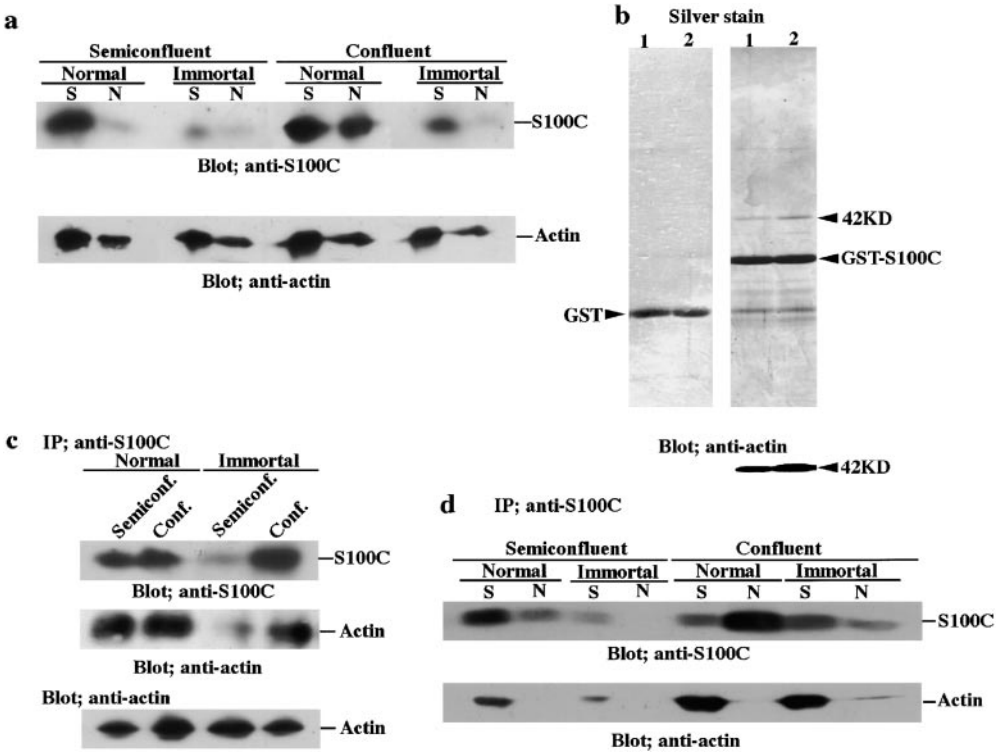

Figure 2. Association of S100C with actin filaments. (a) Subcellular distribution of S100C and actin filaments in soluble and nuclear fractions was determined by Western blotting. (b) Silver staining of GST-S100C (right) or GST (left) binding proteins in normal (lane 1) and immortalized cells (lane 2). Arrowhead indicates a 42-kD protein that was coprecipitated with GST-S100C, but not GST alone. This protein was identified as actin by Western blotting using rabbit anti-actin antibody (b, bottom). (c and d) Association of S100C with actin filaments in normal and immortalized cells by immunoprecipitation assay. Whole cell lysates (c), and soluble (S) and nuclear (N) fractions (d) from normal and immortalized cells at semiconfluent and confluent stages were immunoprecipitated with rabbit anti-S100C antibody. These immunoprecipitates were separated on 15% tricine SDS-PAGE and transferred to nitrocellulose membranes and subjected to the reaction with rabbit anti-actin antibody (c, middle and bottom; d, bottom) and rabbit anti-S100C antibody (c, top; d, top). Total amounts of actin in whole cell lysates were determined by Western blot analysis using rabbit anti-actin antibody (c, bottom).

lecular mass of 42 kD in eluates from the GST-S100C column (Fig. 2 b, top right) but not from the control GST column (Fig. 2 b, top left). Western blot analysis showed that the GST-S100C binding protein (42 kD) was actin (Fig. 2 b, bottom right). When whole cell lysates from normal and immortalized cells at semiconfluence and confluence were immunoprecipitated with rabbit anti-S100C antibody, actin was coprecipitated with S100C in these lysates (Fig. 2 c). In contrast, neither S100C nor actin was detected in immunoprecipitates prepared with preimmune serum (data not shown). Actin bound to S100C was detected in the soluble fractions from both normal and immortalized cells at semiconfluent and confluent stages but not in the nuclear fractions (Fig. 2 d). These results clearly show that S100C associates with actin filaments in the cytoplasm but not in the nucleus of both types of cells independently of cell density.

Immunofluorescence staining of normal and immortalized semiconfluent cells showed that S100C was distributed in the cytoplasm (Fig. 3, a and b). At confluence, intranuclear distribution of S100C was observed in normal cells but not in immortalized cells (Fig. 3, c and d). Preincubation of anti-S100C antibody with the purified recombinant S100C protein diminished the immunostaining of S100C (Fig. 3, a# and c#). In addition, the cells were not stained with preimmune serum, and this distribution pattern was reproduced with different fixations, such as methanol and acetone fixations (data not shown). These results indicated that the S100C immunostain pattern was specific.

Immunofluorescence staining also demonstrated that S100C was colocalized with actin stress fibers (Fig. 3, e, f, e-a′, and f-b′). In addition, a clear colocalization pattern of S100C with actin filaments was visualized at the leading edge, namely filopodia (Fig. 3, g and h, arrows) and lamellipodia (Fig. 3, i and j, arrows) of cells. The leading edge is known as a region where actin filaments are involved in the formation of pseudopodia such as filopodia and lamellipodia (Burridge et al., 1988; Bretscher, 1991). These findings strongly suggest that S100C interacts with actin filaments.

To determine the physiological significance of the interaction between S100C and actin filaments, we microinjected the S100C expression vector pTracer-EF-A-S100C into the nuclei of immortalized cells that expressed only a small amount of endogenous S100C at a low cell density. After 24 h, we observed drastic morphological changes in the S100C-injected cells. These changes were accompanied by the formation of cell protrusions (Fig. 3 k). No similar changes were observed in the cells injected with an empty vector as a negative control (Fig. 3 l). Immunofluorescence staining of actin showed remarkable accumulation of actin filaments in pseudopodia of the cells injected with the S100C expression vector (Fig. 3, m and n, arrows). We further confirmed that these changes were not due to toxic effects of overexpressed S100C, because these cells were viable as judged by the results of a trypan blue exclusion test (data not shown). These results indicated that S100C could control actin organization and have a significant influence on cell morphology.

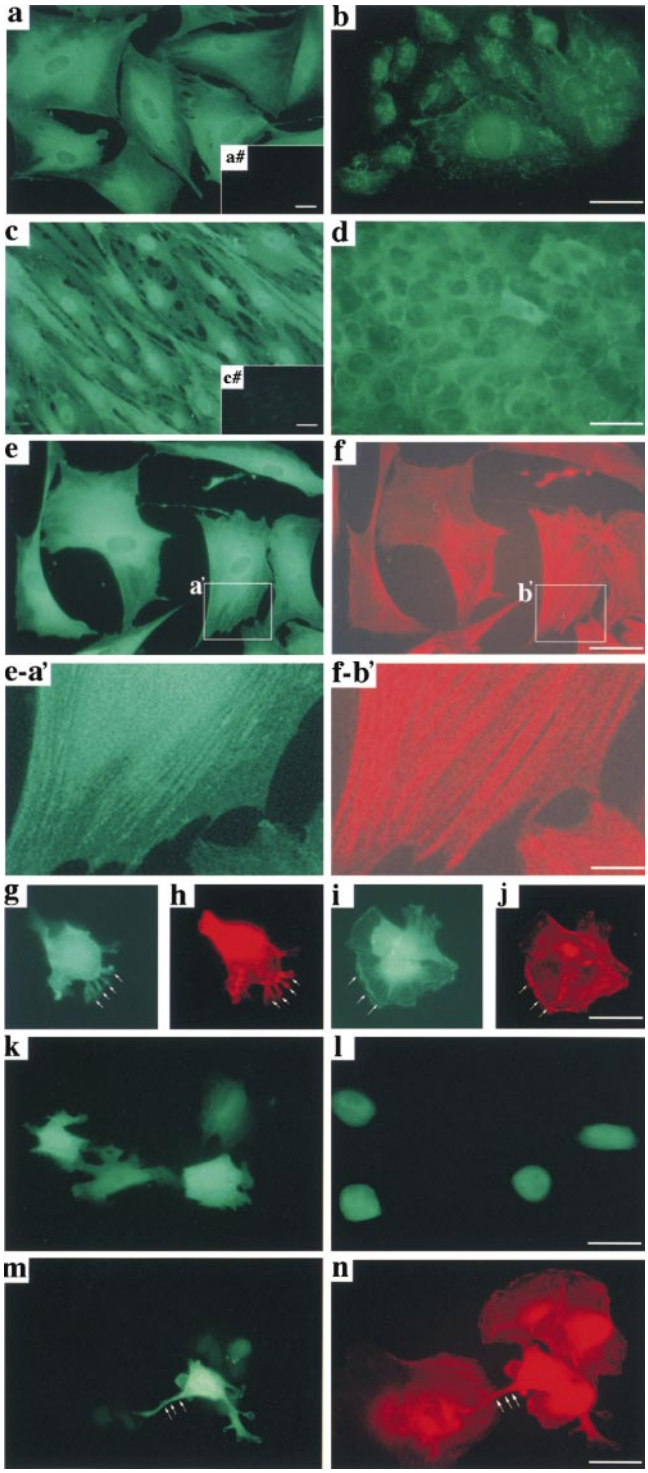

Figure 3. Subcellular localization of S100C in normal KMS-6 and immortalized KMST-6 cells at semiconfluent and confluent stages. S100C was visualized by immunofluorescence staining. (a–d) Normal (a and c) and immortalized cells (b and d) were stained at semiconfluence (a and b) or at confluence (c and d). S100C was detected in the nuclei of normal cells at confluence. Preincubation of anti-S100C antibody with recombinant S100C diminished the immunostaining (a# and c#). (e–j) Double immunofluorescence stainings were performed in normal cells with rabbit anti-S100C antibody (e, e-a′, g, and i) and BODIPY 558/568–conjugated phalloidin (f, f-b′, h, and j). S100C and actin were identified by fluorescence-labeled second antibodies, FITC (green) for S100C, and BODIPY 558/568 (red) for actin, respectively. In interphase cells, the interaction of S100C with actin filaments (e and f) was visualized in cytoplasmic domains (enlarged view of e and f, e-a′, and f-b′). After allowing the cells to attach to and spread on coverslips for 1 h, S100C (g and i) and actin filaments (h and j) were stained in the cells. Arrows show colocalization of S100C and actin filaments at the leading edges of filopodia (g and h) and lamellipodia (i and j). (k–n) Immortalized cells at semiconfluence were microinjected with the S100C expression vector (k, m, and n, pTracer-S100C cDNA) or empty vector (l, pTracer). S100C-expressing (k and m) and -nonexpressing cells (l) were detected by a GFP marker (green) inserted in pTracer, and actin in the cells injected with pTracer-S100C (m) was visualized by BODIPY 558/568–conjugated phalloidin staining (n, red). S100C-expressing cells display a drastic morphological change accompanied by the formation of cell protrusions (k and m) with remarkable accumulation of actin filaments (n, arrows). Bars: 20 μm (b, d, f, l, and m); 5 μm (f-b′); 10 μm (j).

Interaction of S100C with Actin Filaments In Vitro and In Vivo

By coimmunoprecipitation and affinity chromatography, we demonstrated that endogenous S100C actually binds to actin. However, it is not clear what type of actin, for example, G-actin (monomeric actin) or F-actin (actin filaments), associates with S100C. In addition, it remains to be determined whether interaction of S100C with actin is not direct but mediated via an unidentified linker protein(s). Thus, we further investigated the in vitro interaction between S100C and actin filaments by cosedimentation assay.

As shown in Fig. 4 a, when affinity-purified GST-S100C was added to G-actin before its polymerization reaction, GST-S100C was directly incorporated into actin filaments assembled in a Ca^{2+}-dependent manner, whereas S100C-GST failed to bind to actin filaments in the absence of Ca^{2+}. GST alone was never incorporated into actin filaments. Interaction of S100C-GST with G-actin was evaluated by a coprecipitation assay using G-actin–bound DNase I affinity beads in the presence of 1 mM Ca^{2+}. Fig. 4 b shows that G-actin alone did not associate with GST-S100C even though excessive amounts of S100C-GST were added to the mixture. If S100C and DNase I have the same or overlapping binding sites on the actin monomer, binding of S100C to G-actin may not be observed. This possibility remains to be determined. To decide the molar ratio of an S100C–actin filaments complex, densitometric analysis of the in vitro–assembled complex was done, and the results are shown in Fig. 4 c. The amount of GST-S100C that bound to actin filaments increased in parallel with the amount of GST-S100C added, and the mol:mol ratio of GST-S100C and actin filaments was ~1:1. To further examine the interaction of S100C with actin filaments in cells, recombinant S100C labeled with a fluorescent probe was microinjected into the cytoplasm of normal semiconfluent fibroblasts. After 2 h of incubation, the injected exogenous S100C coexisted with actin filaments in a meshwork structure in the cytoplasm (Fig. 4 d). These results coincide well with the immunofluorescent staining patterns of the endogenous S100C in cells (Fig. 3, e and e-a′). Thus, we concluded that S100C directly interacted with actin filaments in a Ca^{2+}-dependent manner.

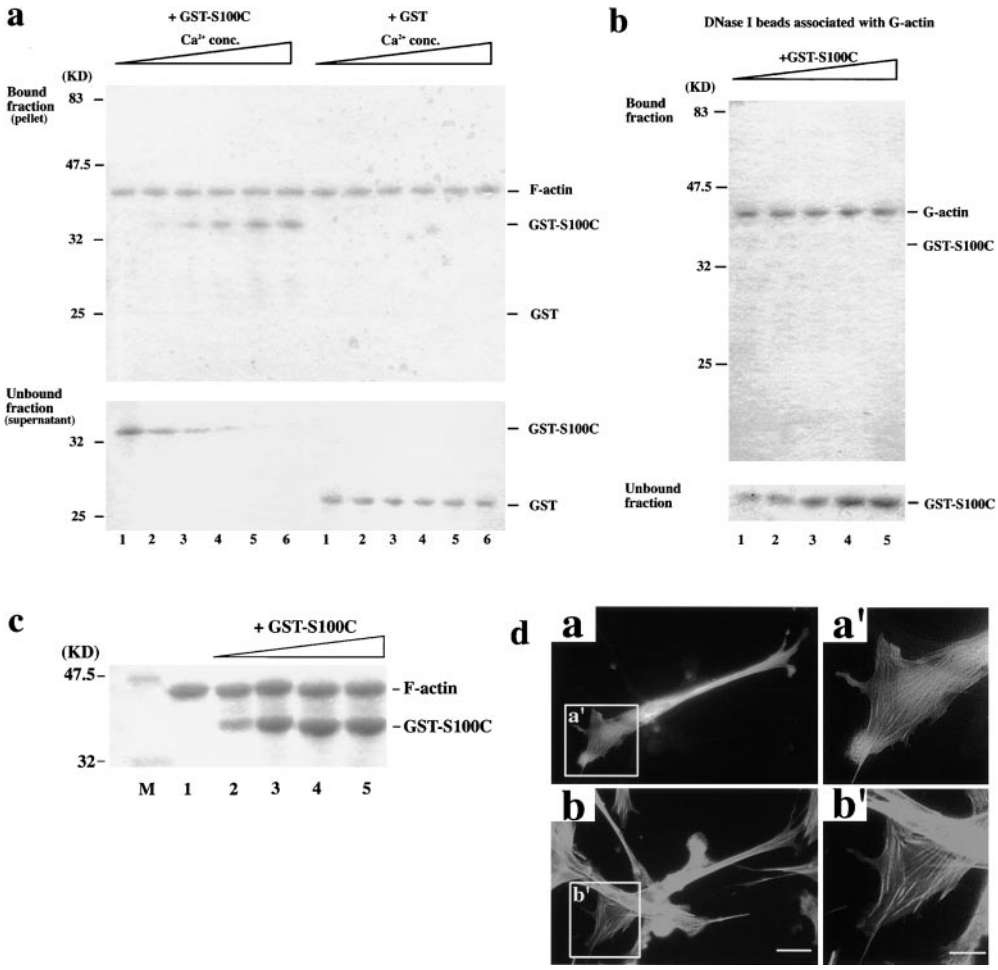

Figure 4. Ca^{2+}-dependent interaction of S100C with actin filaments. (a) In vitro analysis of complex formation between S100C and actin filaments. Recombinant S100C was produced as GST fusion protein in *E. coli* and purified with glutathione-Sepharose beads. Lanes 1–6 show the increasing concentrations of Ca^{2+} (lane 1, 0 M; lane 2, 10^{-7} M; lane 3, 10^{-6} M; lane 4, 10^{-5} M; lane 5, 10^{-4} M; lane 6, 10^{-3} M). Actin filaments (10 μM) were mixed with GST-S100C (10 μM) or GST (10 μM), incubated, and ultracentrifuged. The supernatants and pellets were subjected to SDS-PAGE and analyzed by silver staining. The amount of GST-S100C bound to actin filaments increased in parallel with Ca^{2+} concentration. (b) In vitro analysis of interaction between S100C and G-actin. Various concentrations of GST-S100C (lane 1, 1 μM; lane 2, 5 μM; lane 3, 10 μM; lane 4, 25 μM; lane 5, 50 μM; lane 6, 100 μM) were mixed with DNase I affinity beads coupled with G-actin (10 μM) in the presence of 1 mM Ca^{2+} (the best concentration of Ca^{2+} determined in a) and incubated. After centrifugation, the bead-bound fractions and supernatants (unbound fractions) were analyzed by SDS-PAGE followed by silver staining. S100C did not associate with G-actin. (c) Cosedimentation assay of GST-S100C with actin filaments. Actin filaments (20 μM) were mixed with increasing concentrations of GST-S100C (M, maker; lane 1, 0 μM; lane 2, 10 μM; lane 3, 20 μM; lane 4, 30 μM; lane 5, 40 μM) in the presence of 1 mM Ca^{2+}. After cosedimentation, the pellets were subjected to SDS-PAGE, and each band intensity was densitometrically quantified. The results show that the binding ratio (mol:mol) of GST-S100C and actin filaments is ~1:1. (d) Subcellular localization of exogenous S100C in normal semiconfluent KMS-6 cells. Recombinant S100C labeled with a fluorescent probe was microinjected into the cytoplasm of KMS-6 cells. Localization of exogenous S100C was evaluated by observation under a fluorescent microscope. The exogenous S100C (a and a′) was colocalized with actin filaments (b and b′) in the cytoplasm. a′ and b′ show enlarged views of a and b, respectively. Bars: 20 μm (b); 5 μm (b′).

Movement of S100C into Nuclei of Normal Cells at Confluence

The nuclear localization of S100C in permeabilized normal cells was not affected by the addition of extracts of immortalized cells at semiconfluent (Fig. 5 a, panel I) and confluent stages (Fig. 5 a, panel II). When immortalized confluent cells were permeabilized with digitonin and incubated with the extracts of normal semiconfluent cells, S100C still remained in the cytoplasm (Fig. 5 a, panel III). However, S100C in immortalized confluent cells moved into the nuclei when the cells were permeabilized and incubated with the extracts of normal confluent cells (Fig. 5 a, panel IV). These results indicate that S100C can move from the cytoplasm into the nucleus of normal cells at confluence, but that this motility of the protein is lost in immortalized cells. In other words, cytoplasmic localization of S100C in immortalized cells does not depend on the nuclear exclusion capacity of S100C in the cells.

Interestingly, S100C was phosphorylated only in normal confluent cells (Fig. 5 b). This phosphorylation was markedly reduced by treatment of the cell extracts with alkaline phosphatase (an *E. coli* enzyme, 4 U) at 37°C for 1 h (Fig. 5 c). In addition, electrophoretic separation in the native condition followed by immunoblotting with S100C antibody revealed three (large, middle, and small) protein bands in normal semiconfluent cells as well as immortalized cells at semiconfluent and confluent stages (Fig. 5 d). However, the middle band was lost in normal confluent cells (Fig. 5 d). The middle band reappeared when normal confluent cell extracts were treated with alkaline phosphatase. When the normal confluent cell extracts were added to permeabilized immortalized cells, S100C moved

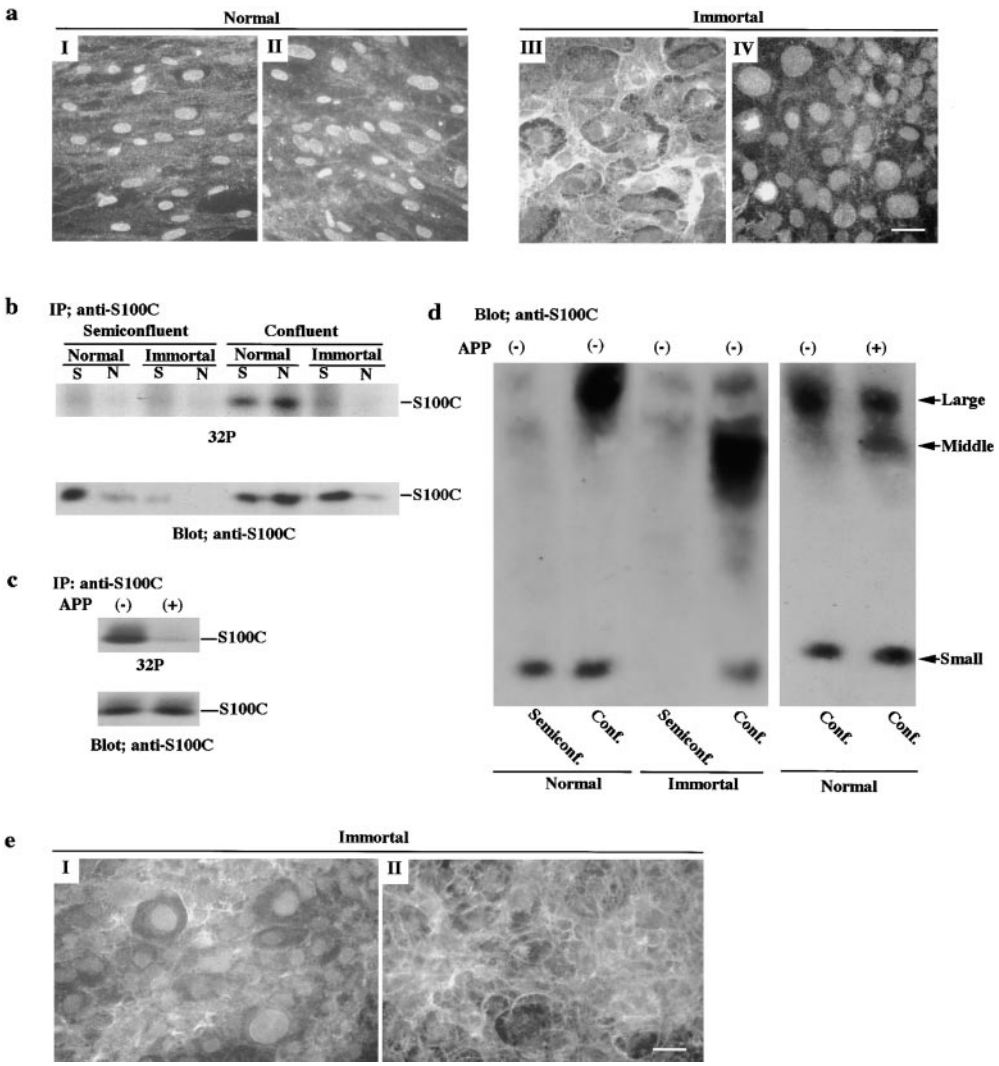

Figure 5. Phosphorylation and nuclear accumulation of S100C. (a) Confluent normal (panels I and II) and immortalized cells (panels III and IV) were permeabilized by treatment with digitonin. These permeabilized cells were incubated with extracts of immortalized (panels I and II) or normal cells (panels III and IV). The extracts were prepared from semiconfluent (panels I and III) and confluent cultures (panels II and IV). S100C in the permeabilized cells treated with various cell extracts was visualized with rabbit anti-S100C antibody as the primary antibody and FITC-conjugated goat anti–rabbit IgG antibody as the secondary antibody. Immortalized cell extracts had no effect on localization of S100C in normal confluent cells (panels I and II). Extracts of normal confluent cells caused nuclear transition of S100C in the immortalized cells at confluence (panel IV), but normal semiconfluent cell extracts had no effect (panel III). Bar, 20 μm. (b) Cells were incubated with [^{32}P]orthophosphate, and soluble (S) and nuclear (N) fractions of the cells were then immunoprecipitated with rabbit anti-S100C antibody. Immunoprecipitates were separated on 15% tricine SDS-PAGE and transferred to nitrocellulose membranes. Phosphorylated S100C was detected by autoradiography (upper). Immunoprecipitated S100C was detected by Western blotting (lower). (c) Whole cell lysates from normal confluent cells were treated with (+) or not treated with (−) alkaline phosphatase (APP). Phosphorylation of S100C in whole cell lysates was markedly reduced by treatment of the lysates with APP (upper). Immunoprecipitated S100C was detected by Western blotting (lower). (d) Native PAGE Western blot analysis of S100C protein complex in whole cell lysates from normal and immortalized cells at semiconfluent and confluent stages. The cell lysates treated with (+) or not treated with (−) APP were subjected to 4% native PAGE and immunoblotted with rabbit anti-S100C antibody. (e) Normal confluent cell extracts were treated with (panel II) or not treated with APP (panel I). APP-treated extracts did not cause nuclear transition of S100C in the permeabilized-immortalized cells at confluence (panel II). Bar, 20 μm.

into the nucleus, whereas the protein remained in the cytoplasm when alkaline phosphatase pretreated extracts were added (Fig. 5 e). These results indicate that the S100C in normal cells is phosphorylated specifically at the confluent stage, forms a complex with unidentified protein(s) (Fig. 5 d, large band), and moves into the nucleus.

Physiological Significance of Phosphorylation of Threonine 10 in S100C

We attempted to determine which amino acid(s) of S100C in normal fibroblasts were phosphorylated in response to high cell density. Furthermore, in order to determine whether endogenous and recombinant S100Cs were phosphorylated at the same or at distinct site(s), we performed 2-D separation of lysylic fragments of immunoprecipitated ^{32}P-labeled endogenous S100C and ^{32}P-labeled recombinant S100C. As shown in Fig. 6 a, only one peptide derived from endogenous S100C was phosphorylated (Fig. 6 a, left panel, NC1), and the same was true of recombinant S100C (Fig. 6 a, right panel, NR1). Locations of phosphopeptide spots NC1 and NR1 were completely consistent, indicating that endogenous and recombinant S100Cs are phosphorylated at the same site. To identify the phosphopeptide, we performed NH_2-terminal sequence analysis of the peptide. As a result, both the sequences of phosphopeptides (NC1 and NR1) were ISSPTETERCIESLIAVFQK (data not shown). Phosphoamino acid analysis of ^{32}P-labeled S100C

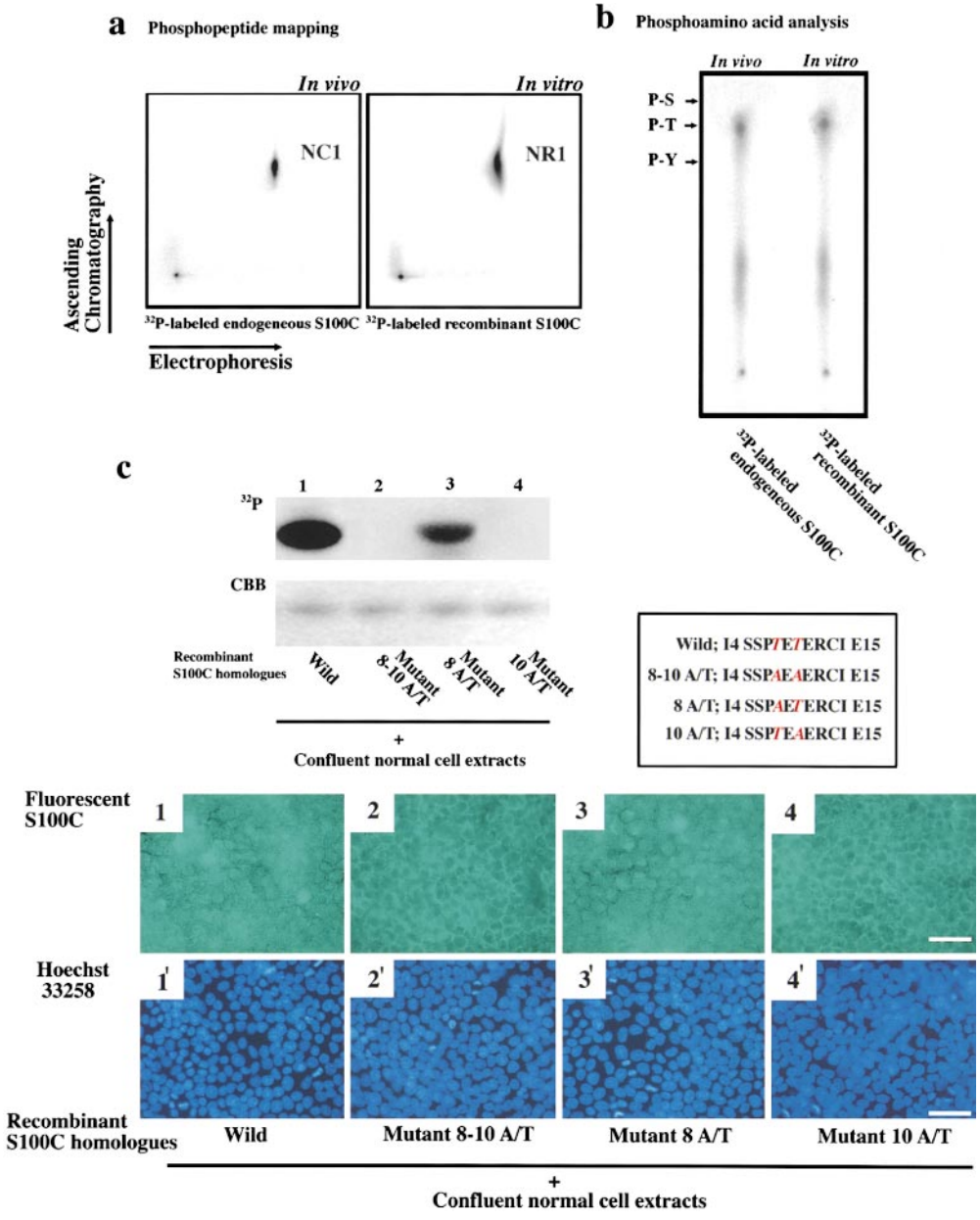

Figure 6. Necessity of phosphorylation of S100C on threonine 10 for nuclear import. (a) Comparative peptide mapping of phosphorylated S100C. In vivo (left panel) and in vitro (right panel) phosphorylations of S100C (endogenous and recombinant S100Cs) were performed as described in Materials and Methods. Peptides from lysyl endopeptidase-treated ^{32}P-labeled endogenous S100C (left panel) or ^{32}P-labeled recombinant S100C (right panel) were prepared and were separated by electrophoresis and ascending chromatography. Each spot named NC1 (in vivo condition, left panel) and NR1 (in vitro condition, right panel) was detected for endogenous or recombinant phosphorylated S100C, respectively. Peptide sequences of both NC1 and NR1 were completely identical, i.e., ISSPTETERCIESLIAVFQK. This peptide indicates the phosphorylation site of S100C in normal cells in response to high cell density. (b) Phosphoamino acid analysis of S100C. Phosphoamino acid analysis of ^{32}P-labeled S100C was performed by the acid hydrolysis method. ^{32}P-labeled phosphothreonine was detected in both in vivo (left) and in vitro (right) conditions after exposure for 1 wk. Samples were spotted at the bottom of thin layer plates. The mobilities of phosphotyrosine (P-Y), phosphothreonine (P-T), and phosphoserine (P-S) standards are indicated at the left vertical axis. Threonine was the amino acid phosphorylated in S100C. (c) Phosphorylation and nuclear accumulation of S100C. Various purified recombinant S100C homologues (wild-type S100C, 8-10 A/T S100C, 8 A/T S100C, and 10 A/T S100C) were labeled with a fluorescent probe as described in Materials and Methods. In vitro phosphorylation reactions of these labeled homologues were performed (upper panel). These ^{32}P-labeled recombinant S100C homologues were subjected to SDS-PAGE and detected by autoradiography (upper panel, top) or CBB staining (upper panel, bottom). Wild-type S100C (lane 1) and 8 A/T S100C (lane 3) were strongly phosphorylated by coincubation with confluent normal cell homogenates, but 8-10 A/T S100C (lane 2) and 10 A/T S100C (lane 4) were not phosphorylated under the same conditions. Confluent HeLa cells permeabilized with digitonin (lower panel, 1–4 and 1′–4′) were incubated with various reaction mixtures (upper panel, lanes 1–4). Exogenously added fluorescent S100C homologues in the permeabilized cells were visualized under a fluorescent microscope (lower panel, 1–4). Nuclei of the permeabilized cells were stained with Hoechst 33258 (lower panel, 1′–4′). Treatment with extracts of confluent normal cells caused nuclear transition of the wild-type S100C (lower panel, 1 and 1′) and the 8 A/T S100C (bottom panel, 3 and 3′) in the permeabilized cells, but the nonphosphorylation type 8-10 A/T (lower panel, 2 and 2′) and 10 A/T S100C (lower panel, 4 and 4′) were not imported into the nuclei. Bars, 20 μm.

showed that threonine was phosphorylated in endogenous S100C (Fig. 6 b, left). When recombinant S100C was incubated with confluent normal cell lysates, threonine residues were also phosphorylated (Fig. 6 b, right). These results indicate that S100C is phosphorylated on threonine residue(s) of the NH_2-terminal 20–amino acid fragment ISSP***T***E***T***ERCIESLIAVFQK (I4-K23 region) in vivo and in vitro.

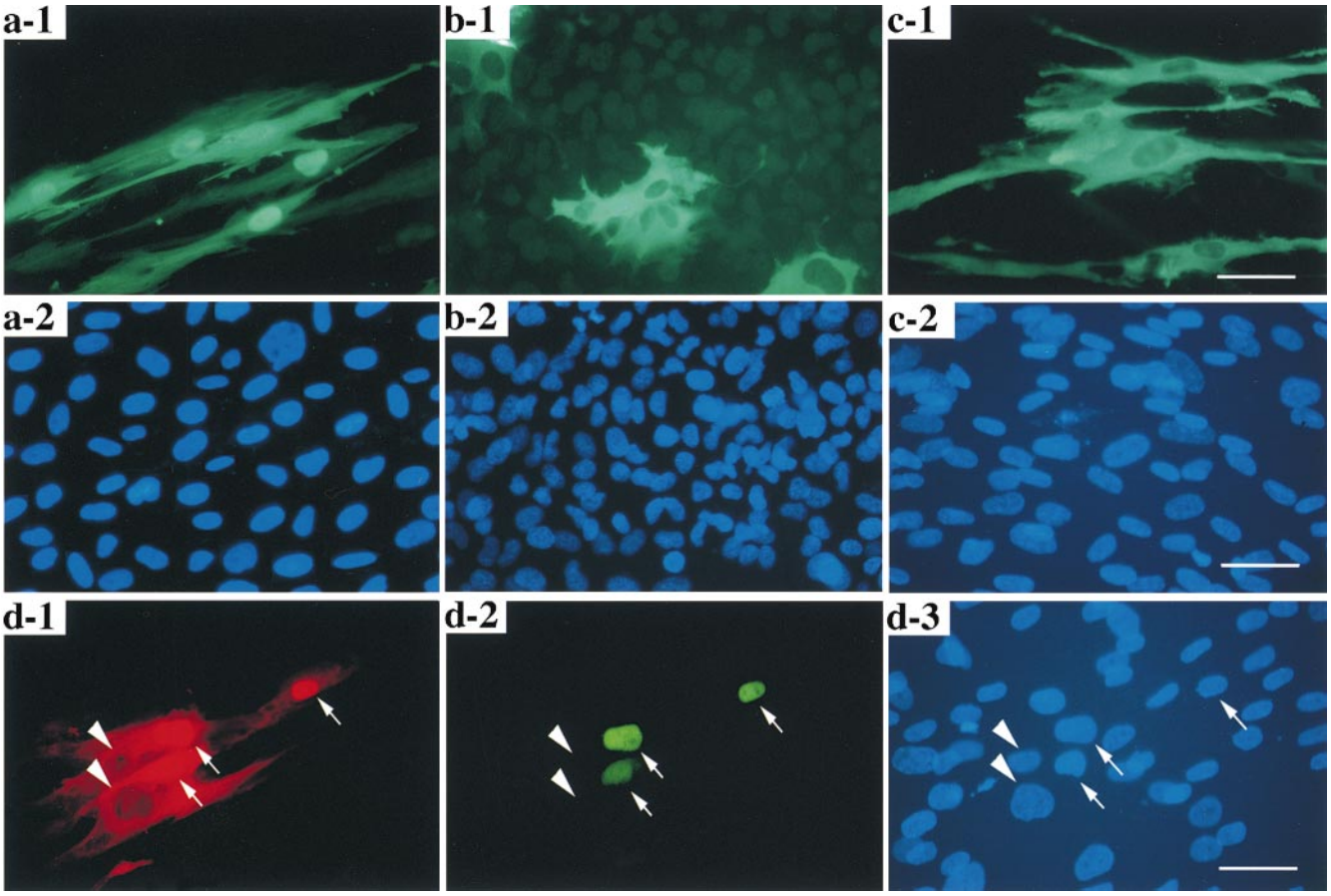

Figure 7. Effect of rabbit anti-S100C antibody on DNA synthesis in normal quiescent cells at confluence. (a–c) Rabbit anti-S100C (a and b) and anti-albumin (c) antibodies were injected into the cytoplasm of normal (a and c) and immortalized cells (b) at confluence. Localization of rabbit anti-S100C antibody in the injected cells was detected with FITC-conjugated goat anti–rabbit IgG antibody (a-1, b-1, and c-1, green). Nuclei were stained with Hoechst 33258 (a-2, b-2, and c-2, blue). (d) Rabbit anti-S100C antibody was microinjected into the cytoplasm of normal quiescent cells at confluence (d-1, d-2, and d-3). Localization of rabbit anti-S100C antibody in the injected cells was visualized in the nuclei (arrows) and the cytoplasm (arrowheads) with TRITC-conjugated goat anti–rabbit IgG antibody (d-1, red). 24 h after injection, DNA synthesis was assessed by immunofluorescence staining with mouse anti-BrdU antibody (d-2, green, arrows). Nuclei were stained with Hoechst 33258 (d-3, blue). Bars, 20 μm.

Our findings raise the possibility that the phosphorylation site may be important for nuclear import of S100C. To test whether this phosphorylation regulates nuclear localization of S100C, we produced three recombinant S100C protein homologues lacking the phosphorylation sites of the I4-K23 region. The threonines 8 (***T8***; bold italics) and 10 (***T10***; bold italics) were changed to alanine (8-10 A/T S100C), and ***T8*** alone (8 A/T S100C) or ***T10*** alone (10 A/T S100C) was changed to alanine. As shown at the top of Fig. 6 c, we found that wild-type S100C and mutant-type 8 A/T, but not 8-10 A/T S100C or 10 A/T S100C, were phosphorylated by incubation with confluent normal cell lysates. Thus, ***T10*** was the primary site of phosphorylation in normal cells at high cell density.

We further investigated nuclear movement of exogenous recombinant S100C homologues that were added to the confluent permeabilized HeLa cells. Unlike the wild-type protein, the mutants (8-10 A/T S100C and 10 A/T S100C) showed almost entirely extranuclear localization (Fig. 6 c, lower panel). The mutant 8 A/T S100C was localized in the nuclei (Fig. 6 c, lower panel). Thus, we found that the phosphorylation on a ***T10*** is necessary to direct S100C to the nucleus.

To determine whether endogenous S100C can move from the cytoplasm into the nucleus under normal physiological conditions, we microinjected rabbit anti-S100C antibody or anti-albumin antibody (a non–cross-reactive IgG against S100C) directly into the cytoplasm of living normal cells at confluence. Consequently, rabbit anti-S100C antibody entered the nuclei of the injected cells at a frequency of 85% (Fig. 7, a-1 and a-2), whereas anti-albumin antibody injected into the cytoplasm did not (Fig. 7, c-1 and c-2). These results indicate that the nuclear envelope was intact and that the rabbit anti-S100C antibody bound to S100C moved into the nucleus from the cytoplasm. Contrarily, when the rabbit anti-S100C antibody was injected into the cytoplasm of immortalized cells at confluence, the antibody remained in the cytoplasm (Fig. 7, b-1 and b-2). It is well known that the antibody cannot go through nuclear pores due to its large size. Therefore, the present results

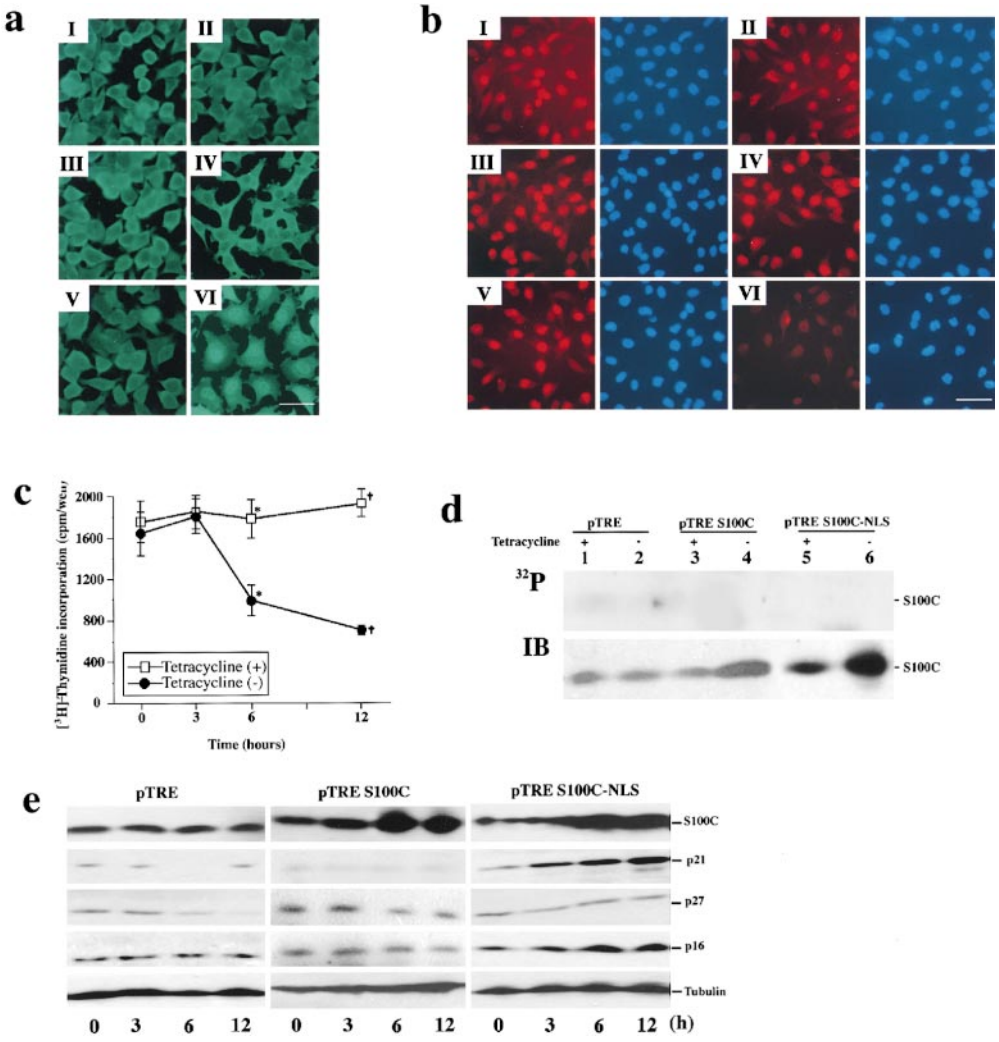

Figure 8. Association of nuclear S100C with cell growth arrest. Localization of S100C (a) and incorporation of BrdU (b) in Tet-off HeLa cells transfected with pTRE S100C-NLS were assessed by immunofluorescence staining. Semiconfluent Tet-off HeLa cells transfected with the empty vector alone (a, panels I and II; b, I and II), with pTRE S100C (a, panels III and IV; b, panels III and IV), and with pTRE S100C-NLS (a, panels V and VI; b, panels V and VI) were stained for S100C or BrdU under tetracycline-plus (a, panels I, III, and V, green; b, panels I, III, and V, left, red) and -minus (a, panels II, IV, and VI, green; b, panels II, IV, and VI, left, red) conditions. When tetracycline was removed from the medium, S100C was detected in the nuclei of Tet-off HeLa cells transfected with pTRE S100C-NLS (a, panel VI, green), and their BrdU incorporation was remarkably decreased (b, panel VI, red). Nuclei were simultaneously stained with Hoechst 33258 (b, panels I–VI, right, blue). Bars, 20 μm. (c) Tritiated thymidine incorporation by Tet-off HeLa cells transfected with pTRE S100C-NLS was assessed under tetracycline-plus and -minus conditions. After deprivation of tetracycline in the medium, DNA synthesis decreased in a time-dependent manner. (d) 6 h after deprivation of tetracycline from the culture medium, transfected cells were further incubated with [^{32}P]orthophosphate for 6 h, and the cells were then immunoprecpitated with rabbit anti-S100C antibody. Phosphorylated S100C was detected by autoradiography (upper). Immunoprecipitated S100C was detected by Western blotting (lower). Phosphorylation of S100C in these cells was not observed. (e) Under the condition of deprivation of tetracycline in the culture medium, the expressions of three cyclin-dependent kinase inhibitors, p21^{Waf1}, p27^{Kip1}, and p16^{Ink4a}, were analyzed in semiconfluent Tet-off HeLa cells transfected with the pTRE empty vector (left), and the pTRE S100C (middle) and pTRE S100C-NLS expression vectors (right) by Western blotting. (Lanes 1–4) 0, 3, 6, and 12 h after deprivation of tetracycline, respectively.

suggest that S100C in living normal cells at confluence can move from the cytoplasm into the nucleus but that S100C in immortalized cells cannot.

Involvement of Nuclear S100C in the Cell Growth Arrest

Anti-S100C antibody was microinjected into the cytoplasm of normal quiescent cells at confluence to determine the biological significance of nuclear accumulation of S100C. Only when the injected anti-S100C antibody formed a complex with S100C protein and moved into nuclei (Fig. 7, d-1 and d-3, arrows) did the cells incorporate BrdU into their nuclei (Fig. 7, d-2 and d-3, arrows). On the other hand, cytoplasmic injection of anti-albumin antibody or IgG fraction prepared from preimmune serum showed no movement of the antibody into their nuclei and did not induce the incorporation of BrdU (data not shown). Since blocking the intranuclear S100C functions with anti-S100C antibody that entered the nucleus caused DNA synthesis in quiescent cells, nuclear accumulation of S100C may be closely related to inhibition of DNA synthesis in normal human fibroblasts at confluence.

To further evaluate the association of nuclear S100C with the cell growth arrest, we employed a Tet-on/off gene expression system. Since the endogenous S100C in Tet-off HeLa cells was localized only in the cytoplasm, the exogenous S100C may also be localized in the cytoplasm. An NLS was linked to S100C by a PCR technique to compel exogenous S100C to move into the nucleus. Tet-off HeLa cells were transfected with an empty vector, pTRE (Fig. 8 a, panels I and II and Fig. 8 b, panels I and II), or an ex-

pression vector of wild-type S100C, pTRE S100C (Fig. 8 a, panels III and IV and Fig. 8 b, panels III and IV), or an expression vector of S100C-NLS fusion protein, pTRE S100C-NLS (Fig. 8 a, panels V and VI and Fig. 8 b, panels V and VI). Clones overexpressing wild-type S100C or S100C-NLS under a tetracycline-free condition were isolated and analyzed. The expression levels of S100C or S100C-NLS proteins in the clones, Tet-off HeLa/pTRE S100C, and Tet-off HeLa/pTRE S100C-NLS, were seven and ten times higher than the basal level in the control Tet-off HeLa/pTRE clone, respectively (Fig. 8 d, lower). Immunocytochemical studies revealed that when tetracycline was deprived from the medium (Fig. 8 a, panels II, IV, and VI and Fig. 8 b, II, IV, and VI), exogenous S100C-NLS protein expressed in the transfected cells efficiently moved to and accumulated in the nuclei (Fig. 8 a, panel VI). However, the overexpressed wild-type S100C did not move into the nuclei (Fig. 8 a, panel IV). Although neither S100C nor S100C-NLS was phosphorylated (Fig. 8 d, upper), the latter protein could move into the nuclei because of the presence of NLS. Interestingly, the S100C-NLS–overexpressing cells displayed more flattened morphology (Fig. 8 a, panel VI) as compared with the cells under the tetracycline-plus condition (Fig. 8 a, panel V) and their mother cells (Fig. 8 a, panels I and II). On the other hand, the wild-type S100C-overexpressing cells showed polygonal morphology with some protrusions (Fig. 8 a, panel IV). Then, DNA synthesis was assessed in the Tet-off HeLa/pTRE S100C-NLS clone by incorporation of BrdU or [^{3}H]thymidine. BrdU staining revealed that DNA synthesis was inhibited by nuclear accumulation of the fusion protein (Fig. 8 b, panel VI), whereas the wild-type S100C-expressing cells continued to synthesize DNA under the deprivation of tetracycline in the culture medium (Fig. 8 b, panel IV). This inhibition was time-dependent after deprivation of tetracycline in the culture medium, and the maximum inhibition was ~50% at 12 h (Fig. 8 c).

Expression of cyclin-dependent kinase inhibitors such as $p21^{Waf1}$ and $p16^{Ink4a}$ was tested in the Tet-off HeLa/pTRE S100C-NLS clone. As shown in Fig. 8 e, both $p21^{Waf1}$ and $p16^{Ink4a}$ were remarkably induced as early as 3 h after the deprivation of tetracycline in parallel with the expression of exogenous S100C-NLS, whereas $p27^{Kip1}$ level did not change. The overexpression of exogenous wild-type S100C had no effect on the expression of $p21^{Waf1}$ and $p16^{Ink4a}$.

Discussion

Association of Cytoplasmic S100C with the Regulation of Actin Organization and Its Dynamics

In this study, we found that S100C was remarkably downregulated in immortalized cells at low cell density as compared with their normal counterparts, and that S100C was directly associated with actin filaments in the cytoplasm in normal and immortalized cells. Furthermore, we observed that high expression of exogenous S100C caused drastic changes in the morphology of immortalized cells at low cell density. This morphological change was associated with the formation of cell protrusions with densely organized actin filaments. Thus, it is likely that cytoplasmic S100C is implicated in the regulation of actin organization and actin filament dynamics. Intracytoplasmic injection of anti-S100C antibody caused multinucleation in most of the injected normal fibroblasts at low cell density (data not shown). In addition, multinucleated cells were often observed in cultures of immortalized cells at low cell density. Thus, formation of the S100C immunocomplex may lead to the abnormal formation of actin contractile ring in cytokinesis (Haraguchi et al., 1997).

Nuclear Accumulation of S100C and Cell Density–dependent Growth Arrest

Normal human fibroblasts go into the stage of growth arrest at confluence. However, little is known about the molecular mechanism underlying this phenomenon. As a clue to resolve this matter, it is important to understand how the information of growth arrest is transported from the cell–cell contact sites into the nucleus, where the on/off switch of several gene expression systems related to growth arrest are present. In other words, sites of cell–cell contact regions may represent signaling hotspots on the cell surface.

S100C was phosphorylated in normal human fibroblasts at high cell density. Interestingly, S100C was released from actin filaments when S100C was specifically phosphorylated on threonine 10. In other words, the binding ability of S100C to actin filaments was extremely diminished by the phosphorylation even in the presence of a high concentration of Ca^{2+} (data not shown). Phosphorylated S100C was accumulated in the nuclei of normal human fibroblasts. This result may be reasonable for the nuclear import mechanism of S100C because it may be impossible for S100C to move into the nucleus if the protein remains to be linked to actin filaments in the cytoplasm. Thus, dissociation of S100C from actin filaments may be one factor involved in the nuclear import mechanism of the protein.

In immortalized cells, S100C was neither phosphorylated nor imported to the nucleus. Thus, phosphorylation of S100C on threonine 10 may be essential to import into the nucleus through interaction with putative S100C-binding protein(s) containing an NLS (Dingwall and Laskey, 1991) and to contribution to the cell density–dependent growth arrest. In fact, when the phosphorylated S100C in normal cell lysates from confluent culture was dephosphorylated by treatment of the lysates with alkaline phosphatase, the nuclear import of S100C was markedly diminished. Furthermore, recombinant S100C protein homologues lacking the phosphorylation site never localized in the nucleus. Thus, we emphasize that the phosphorylation on threonine 10 is necessary for the cytoplasmic S100C to move to the nucleus. Since we did not find the NLS sequence in S100C by examining the amino acid sequence of this protein, we suppose that phosphorylated S100C could be associated with an unknown NLS-bearing protein and then their complex could move into the nucleus through interaction with nuclear transporters, such as importin-α (Gorlich et al., 1994; Moroianu et al., 1995; Weis et al., 1995) and importin-β (Chi et al., 1995; Radu et al., 1995; Cingolani et al., 1999).

Nuclear accumulation of S100C seems to be closely related to cell density–dependent growth arrest in cultures of normal human fibroblasts. The neoplastic cells such as

HeLa, KMST-6/Ras, and Saos-2 cells show no contact inhibition of growth. Therefore, we hypothesized that nuclear import of S100C could not occur in neoplastic cells. In fact, we found that S100C was localized only in the cytoplasm of neoplastic HeLa, KMST-6/Ras, and Saos-2 cells, and that the phosphorylation of S100C in these cells did not occur even after confluence (data not shown). Thus, disorder of the nuclear import mechanisms of S100C may impair cell density–dependent growth arrest in immortalized and neoplastic cells at confluence.

To clarify the relationship between nuclear accumulation of S100C and cell growth arrest, we transfected Tet-off HeLa cells with a plasmid pTRE S100C-NLS. Under deprivation of tetracycline in the culture medium, the transfected cells stably expressed significant amount of S100C-NLS fusion protein which was not phosphorylated but accumulated in the nuclei of the transfected Tet-off HeLa cells. By this approach, it became clear that accumulation of S100C-NLS in the nuclei of HeLa cells significantly inhibited DNA synthesis of the cells. Interestingly, expression of both $p21^{Waf1}$ and $p16^{Ink4a}$, the well known inhibitors of cyclin-dependent kinases (Hunter, 1993; Serrano et al., 1993), was increased in parallel with the nuclear accumulation of S100C. These results indicate that $p21^{Waf1}$ and $p16^{Ink4a}$ may mediate downregulation of DNA synthesis by the nuclear S100C. Thus, whenever cytoplasmic S100C is artificially compelled to move into the nucleus, S100C can act as a mediator of the cell-cycle arrest independently of its phosphorylation or nonphosphorylation conditions. However, naturally, when the phosphorylation of S100C does not occur in the cytoplasm, S100C can neither move into the nucleus nor act as a cell-cycle downregulator. Consequently, we conclude that the phosphorylation of S100C is necessary for the nuclear import and the following suppression of DNA synthesis in cells.

It is clear that S100C shuttles between the cytoplasm and the nucleus of normal human fibroblasts in a cell density–dependent fashion. Recent studies also have demonstrated that the same proteins reside both at adherent junctions and in the nucleus. For example, the tight junction protein ZO-1 accumulates in the nucleus in a cell density–dependent fashion (Gottardi et al., 1996), and the focal contact protein Zyxin shuttles between the nucleus and the sites of cell adhesion in fibroblasts (Nix and Beckerle, 1997).

β-Catenin, a protein present at cell–cell adherent junctions, has been shown to work as a DNA-binding transcriptional regulator when β-catenin–Lef-1 transcription factor complex accumulates in the nucleus (Gumbiner, 1995; Behrens et al., 1996; Huber et al., 1996; Orsulic and Peifer, 1996). Recently, Carrión et al. (1999) have reported that DREAM (downstream regulatory element [DRE]-antagonist modulator), an EF-hand type Ca^{2+}-binding protein, binds to the DRE sequence and acts as a location-dependent gene silencer of the human *prodynorphin* gene. Thus, the structure of the EF-hand helix-loop-helix motif domain appears to be compatible with a nucleic acid–binding function. In fact, we found that both cellular S100C and recombinant S100C protein bound to double-stranded DNA coupled with a cellulose column (data not shown). Like DREAM, the EF-hand type Ca^{2+}-binding protein S100C may also work as a DNA-binding transcriptional regulator for cell density–dependent growth arrest.

Submitted: 27 December 1999
Revised: 4 May 2000
Accepted: 4 May 2000

References

Allen, B.G., I. Durussel, M.P. Walsh, and J.A. Cox. 1996. Characterization of the Ca^{2+}-binding properties of calgizzarin (S100C) isolated from chicken gizzard smooth muscle. *Biochem. Cell Biol.* 74:687–694.

Bai, L., K. Mihara, Y. Kondo, M. Honma, and M. Namba. 1993. Immortalization of normal human fibroblasts by treatment with 4-nitroquinoline 1-oxide. *Int. J. Cancer.* 53:451–456.

Behrens, J., J.P. Von Kris, M. Kunl, L. Bruhn, D. Wedlich, R. Grosschedl, and W. Birchmeier. 1996. Functional interaction of β-catenin with the transcription factor LEF-1. *Nature.* 382:638–642.

Bretscher, A. 1991. Microfilament structure and function in the cortical cytoskeleton. *Annu. Rev. Cell Biol.* 7:337–374.

Burridge, K., K. Fath, T. Kelly, G. Nuckolls, and C. Turner. 1988. Focal adhesions: transmembrane junctions between the extracellular matrix and the cytoskeleton. *Annu. Rev. Cell Biol.* 4:487–525.

Carrión, A.M., W.A. Link, F. Lego, B. Mellström, and J.R. Naranjo. 1999. DREAM is a Ca^{2+}-regulated transcriptional repressor. *Nature.* 396:80–84.

Chi, N.C., E.J.H. Adam, and S.A. Adam. 1995. Sequence and characterization of cytoplasmic nuclear import factor p97. *J. Cell Biol.* 130:265–274.

Cingolani, G., C. Petosa, K. Weis, and C.W. Muller. 1999. Structure of importin-β bound to the IBB domain of importin-α. *Nature.* 399:221–229.

Dingwall, C., and R.A. Laskey. 1991. Nuclear targeting sequences: a consensus? *Trends Biochem. Sci.* 16:178–181.

Dover, R., and K. Patel. 1994. Improved methodology for detecting bromodeoxyuridine in cultured cells and tissue sections by immunocytochemistry. *Histochemistry.* 102:383–387.

Fackler, M.J., C.I. Civin, D.R. Sutherland, M.A. Baker, and W.S. May. 1990. Activated protein kinase C directly phosphorylates the CD34 antigen on hematopoietic cells. *J. Biol. Chem.* 239:243–253.

González, M., V. Cambiazo, and R. Maccioni. 1998. The interaction of Mip-90 with microtubules and actin filaments in human fibroblasts. *Exp. Cell Res.* 239:243–253.

Gorlich, D., S. Prehn, R.A. Laskey, and E. Hartmann. 1994. Isolation of a protein that is essential for the first step of nuclear import. *Cell.* 79:767–778.

Gottardi, C.J., M. Arpin, A.S. Fanning, and D. Louvard. 1996. The junction-associated, ZO-1, localizes to the nucleus before the maturation and during the remodeling of cell-cell contacts. *Proc. Natl. Acad. Sci. USA.* 93:10779–10784.

Gumbiner, B.M. 1995. Signal transduction of β-catenin. *Curr. Opin. Cell Biol.* 7:634–640.

Haraguchi, T., T. Kaneda, and Y. Hiraoka. 1997. Dynamics of chromosomes and microtubules visualized by multiple-wavelength fluorescence imaging in living mammalian cells: effects of mitotic inhibitors on cell cycle progression. *Genes Cells.* 2:369–380.

Hayflick, L. 1997. Mortality and immortality at the cellular level. A review. *Biochemistry.* 62:1181–1190.

Huber, O., C. Bierkamp, and R. Kemler. 1996. Cadherins and catenins in development. *Curr. Opin. Cell Biol.* 8:685–691.

Hunter, T. 1993. Braking the cycle. *Cell.* 75:839–841.

Kondo, T., K. Mihara, Y. Inoue, M. Iijima, and M. Namba. 1995. Two-dimensional gel electrophoretic analysis of down-regulated proteins in human fibroblasts immortalized by treatment with either 4-nitroquinoline 1-oxide or ^{60}Co gamma rays. *Electrophoresis.* 16:1067–1073.

Kondo, T., M. Sakaguchi, and M. Namba. 1998a. Characteristics of intracellular transferrin produced by human fibroblasts: its posttranscriptional regulation and association with tubulin. *Exp. Cell Res.* 242:38–44.

Kondo, T., M. Sakaguchi, H. Yamada, and M. Namba. 1998b. Two-dimensional gel electrophoretic analysis of the changes after immortalization of human cells: decrease of intracellular α-2-macroglobulin fragment. *Electrophoresis.* 19:1836–1840.

Lindeman, G.J., S. Gaubatz, D.M. Livingston, and D. Ginsberg. 1997. The subcellular localization of E2F-4 is cell-cycle dependent. *Proc. Natl. Acad. Sci. USA.* 94:5095–5100.

Marti, T., K.D. Erttmann, and M.Y. Gallin. 1996. Host-parasite interaction in human onchocerciasis: identification and sequence analysis of a novel human calgranulin. *Biochem. Biophys. Res. Commun.* 221:454–458.

Mishra, K., and V.K. Parnaik. 1995. Essential role of protein phosphorylation in nuclear transport. *Exp. Cell Res.* 216:124–134.

Moroianu, J., G. Blobel, and A. Radu. 1995. Previously identified protein of uncertain function is karyopherin-α and together with karyopherin-β docks import substrate at nuclear pore complex. *Proc. Natl. Acad. Sci. USA.* 92:2008–2011.

Naka, M., Z.X. Qing, T. Sasaki, H. Kise, I. Tawara, S. Hamaguchi, and M. Tanaka. 1994. Purification and characterization of a novel calcium-binding protein, S100C, from porcine heart. *Biochem. Biophys. Acta.* 1223:348–353.

Namba, M., K. Nishitani, F. Hyodoh, F. Fukushima, and T. Kimoto. 1985. Neo-

plastic transformation of human diploid fibroblasts (KMST-6) by treatment with ^{60}Co gamma rays. *Int. J. Cancer.* 35:275–280.

Namba, M., K. Nishida, F. Fukushima, and T. Kimoto. 1988. Multi-step neoplastic transformation of normal human fibroblasts by ^{60}Co gamma rays and *Ha-ras* oncogenes. *Mutat. Res.* 8:947–958.

Namba, M., K. Mihara, and K. Fushimi. 1996. Immortalization of human cells and its mechanisms. *Crit. Rev. Oncog.* 7:19–31.

Nix, D.A., and M.C. Beckerle. 1997. Nuclear-cytoplasmic shuttling of the focal contact protein, zyxin: a potential mechanism for communication between sites of cell adhesion and the nucleus. *J. Cell Biol.* 138:1139–1147.

Orsulic, S., and M. Peifer. 1996. An in vivo structure-function study of armadillo, the beta-catenin homologue, reveals both separate and overlapping regions of the protein required for cell adhesion and for wingless signaling. *J. Cell Biol.* 134:1283–1300.

Radu, A., G. Blobel, and M.S. Moore. 1995. Identification of a protein complex that is required for nuclear import and mediates docking of import substrates to distinct nucleoporins. *Proc. Natl. Acad. Sci. USA*. 92:1769–1773.

Rhim, J.S., J.H. Yoo, J.H. Park, P. Thraves, Z. Salehi, and A. Dritschilo. 1990. Evidence for the multistep nature of in vitro human epithelial cell carcinogenesis. *Cancer Res.* 50:5653s–5657s.

Sakaguchi, M., T. Kondo, P. Hong, and M. Namba. 1998. Differential localization of two types of transferrin: produced by human fibroblasts or incorporated from culture medium. *Cell Struct. Funct.* 23:69–72.

Sakaguchi, M., T. Kondo, P. Hong, and M. Namba. 1999. Transferrin synthesized in cultured human fibroblasts is associated with tubulins and has iron binding capacity. *Cell Struct. Funct.* 24:5–9.

Schnekess, B.O., and M.P. Walsh. 1997. Molecular cloning and expression of avian smooth muscle S100A11 (calgizzarin, S100C). *Biochem. Cell Biol.* 75: 771–775.

Scotto, C., J.C. Delouleme, D. Rousseau, E. Chambaz, and J. Baudier. 1998. Calcium and S100B regulation of p53-dependent cell growth arrest and apoptosis. *Mol. Cell. Biol.* 18:4272–4281.

Serrano, M., G.J. Hannon, and D. Beach. 1993. A new regulatory motif in cell-cycle control causing specific inhibition of cyclin D/CDK4. *Nature.* 366:704–707.

Tanaka, M., K. Adzuma, M. Iwami, K. Yoshimoto, Y. Monden, and M. Itakura. 1995. Human calgizzarin; one colorectal cancer-related gene selected by a large scale random cDNA sequencing and northern blot analysis. *Cancer Lett.* 89:195–200.

Tom, T.D., L.H. Malkas, and R.J. Hickey. 1996. Identification of multiprotein complexes containing DNA replication actors by native immunoblotting of HeLa cell protein preparations with T-antigen-dependent SV-40 DNA replication activity. *J. Cell. Biochem.* 63:259–267.

Watanabe, M., Y. Ando, H. Todoroki, H. Minami, and H. Hidaka. 1991. Molecular cloning and sequencing of a cDNA clone encoding a new calcium binding protein, named calgizzarin, from rabbit lung. *Biochem. Biophys. Res. Commun.* 181:644–649.

Weis, K., I.W. Mattaj, and A.I. Lamond. 1995. Identification of hSRP1a as a functional receptor for nuclear localization sequences. *Science.* 268:1049–1053.

Yokoya, F., N. Imamoto, T. Tachibana, and Y. Yoneda. 1999. Beta-catenin can be transported into the nucleus in a Ran-unassisted manner. *Mol. Biol. Cell.* 10:1119–1131.